Pakistan Veterinary Journal

ISSN: 0253-8318 (PRINT), 2074-7764 (ONLINE)
DOI: 10.29261/pakvetj/2026.030

RESEARCH ARTICLE

Polysaccharide of Xizang *Coriolus versicolor* Mitigates Spleen Damage in Mice Exposed to Chromium by Regulating Gut Microbiota

Shixiong Chen[1], Chang Xu[2], Yuqing Huang[3,4*], Qipeng Lv[5], Maha Abdullah Momenah[6], Eman A. Al-Shahari[7] and Kun Li [2*]

[1]Key Laboratory of Traditional Chinese Veterinary Medicine and Animal Health in Fujian Province, College of Animal Sciences, Fujian Agriculture and Forestry University, Fuzhou 350002 China; [2]College of Veterinary Medicine, Nanjing Agricultural University, Nanjing 210095, PR China; [3]Department of Spleen and Gastroenterology, Hubei Provincial Hospital of Traditional Chinese Medicine, Affiliated Hospital of Hubei University of Chinese Medicine, Wuhan 430061, China; [4]Hubei Shizhen Laboratory, Wuhan 430061, China; [5]Xining Wildlife Park, Xining, 810000, China; [6]Department of Biology, College of Science, Princess Nourah bint Abdulrahman University, P.O. Box 84428, Riyadh 11671, Saudi Arabia; [7]Health Specialties, Basic Sciences and Their Applications Unit, Applied College at Muhayil Asir, King Khalid University, Abha, Saudi Arabia
*Corresponding author: lk3005@njau.edu.cn (KL); 429005a00eg.cdb@sina.cn (YH)

ARTICLE HISTORY (25-1193)

Received: December 06, 2025
Revised: January 31, 2026
Accepted: February 02, 2026
Published online: February 04, 2026

Key words:
Chromium
Mice
Microbiota
Polysaccharide
Spleen

A B S T R A C T

Chromium has become increasingly hazard due to its strong carcinogenicity; effective therapeutic options for managing such injuries remain limited. We examined the effect of the polysaccharide of Xizang *Coriolus versicolor* (CV) on spleen damage in mice exposed to chromium. Mice (n=30) were divided into KCH, KMH, and KYH groups. Group KMH and KYH were induced by $K_2Cr_2O_7$ (15 mg/kg), and KYH was administered with 50 mg/kg CV polysaccharide for 35 days. We found that the weight of mice in the KMH group was significantly lower than in the KCH ($P<0.05$) and KYH ($P<0.05$) on the 35th day, while the spleen index in KMH was higher than that of animals in other groups ($P<0.05$). H&E and Sirius red staining showed that hexavalent chromium led to serious atrophy of white pulp and acini lienal, blurry marginal zone, and infiltration of inflammatory cells in mice; however, mice supplemented with CV polysaccharide had clear red and white pulp, fewer inflammatory cells, and decreased fibrosis. CV polysaccharide decreased serum IL-6 ($P<0.01$), IL-1β ($P<0.001$), TNF-α ($P<0.001$), and MDA ($P<0.001$), while increasing IL-10 ($P<0.01$), T-AOC ($P<0.001$), and GSH-Px ($P<0.001$) in mice. Microbiota sequencing achieved 1,383,401 filtered sequences and found two phyla and nine genera with significant differences among the three groups. Genera were *Dwaynesavagella*, *Streptococcus*, *UBA7173*, *QWKK01*, *Bifidobacterium* 388775, *Lactococcus* A 343473, *Gemella,* and *Bacillus* P 294101. In summary, we confirmed that the polysaccharide of Xizang *Coriolus versicolor* could alleviate spleen damage in mice exposed to chromium by regulating inflammatory response, antioxidant capacity, and gut microbiota.

To Cite This Article: Chen S, Xu C, Huang Y, Lv Q, Momenah MA, Eman AA and Li K, 2026. Polysaccharide of Xizang *Coriolus versicolor* mitigates spleen damage in mice exposed to chromium by regulating gut microbiota. Pak Vet J, 46(2): 419-428. http://dx.doi.org/10.29261/pakvetj/2026.030

INTRODUCTION

The density greater than 5 g/cm³ inorganic elements were considered as heavy metals, which include elements such as mercury, lead, copper, and chromium (Kim *et al.,* 2019). Among these, chromium and several others are recognized as non-essential and toxic metals (Bronte and Pittet, 2023). Over the past few decades, chromium has become increasingly notorious due to its strong carcinogenicity (Wise and Wise, 2012). Chromium exists in several oxidation states in the environment, with trivalent chromium (Cr III) and hexavalent chromium (Cr VI) being the most stable and toxic forms (Sharma *et al.,* 2022; Aljohani, 2025). Cr III has been associated with gene mutations and genotoxic effects (Zhang *et al.,* 2008; Wise and Wise, 2012), while Cr VI, a widely used industrial chemical, is known to cause cancer and neurotoxicity (Ma *et al.,* 2022; Wise *et al.,* 2022). These toxicological

concerns have contributed to increasing global attention on chromium as a hazardous environmental pollutant.

The spleen is a vital organ contributing to both innate and adaptive immune responses against pathogenic microorganisms (Zheng *et al.,* 2022). In addition to its immunological role, the spleen also contributes significantly to red blood cell homeostasis and iron metabolism (Bronte and Pittet, 2023). Previous studies have reported lipid peroxidation in the heart, spleen, and lungs of mice exposed to hexavalent chromium (Boşgelmez and Güvendik, 2019), as well as severe tissue damage in chicks subjected to hexavalent chromium exposure (Zhao *et al.,* 2022). Despite the known toxicity of this compound, effective therapeutic options for managing such injuries remain limited.

Mushrooms have long been recognized in China as traditional edible foods with immunoregulatory and health-promoting properties (Jeitler *et al.,* 2020). *Coriolus versicolor* (CV), commonly known as Yunzhi in China, is a medicinal fungus traditionally used to treat symptoms such as loss of appetite, fatigue, and impotence. It is also believed to promote longevity and has recently gained attention for its potential anticancer properties (Saleh *et al.,* 2017; Pilkington *et al.,* 2022). One of its active components, a polysaccharide, exhibits various biological activities, including the regulation of inflammation and immune responses, as well as anti-diabetic and anti-tumor effects (Luo *et al.,* 2014; Saleh *et al.,* 2017; Jing *et al.,* 2022; Saleem *et al.,* 2025).

The intestinal microbiota was composed of all kinds of microorganisms, including bacteria, viruses, and eukaryotes (El-Sayed *et al.,* 2021), which contribute to host health by modulating metabolic processes and immune function (Geng *et al.,* 2022; Sittipo *et al.,* 2022; Yang *et al.,* 2025). Numerous studies have highlighted the potential of microbiota-targeted interventions as novel therapeutic strategies for various diseases, including obesity (Alipour *et al.,* 2022), diabetic kidney disease (Wu *et al.,* 2024), and liver disorders (Albhaisi *et al.,* 2019). *Coriolus versicolor* is a traditional medicinal fungus known for its spleen-tonifying properties (Jing *et al.,* 2022); however, its effects on chromium-induced spleen damage remain largely unexplored. Herein, we tried to investigate the protective effects of the polysaccharide of Xizang *C. versicolor* on chromium-induced spleen injury in mice, with a particular focus on its role in modulating the gut microbiota.

MATERIALS AND METHODS

Ethics statement: All the experimental regulations were approved by the Laboratory Animals Research Centre of Jiangsu, China, and the ethics committee of Nanjing Agricultural University (NJAU.No20240910163).

Polysaccharide extraction: Xizang *Coriolus versicolor* was obtained from Tongrentang Pharmacy (Nanjing, China) for polysaccharide extraction. The fungal material was first ground into a fine powder and mixed with 20 times its volume of 95% ethanol (w/v). This mixture was subjected to ultrasonic treatment for 45 minutes, followed by hot water extraction (10 times the volume, w/v) at 100 °C, conducted twice. To isolate the polysaccharides, proteins were removed from the extract using the Sevag reagent, as reported in a previous study (Chen *et al.,* 2019). The extracted polysaccharides were then freeze-dried into powder form. Their concentration was measured by utilizing the phenol-sulfuric acid method.

Mice experiment: Four-week-old thirty (n=30) Kunming mice were bought from the Experimental Center of Yangzhou University (Yangzhou, China). All mice were housed under standardized conditions at the Laboratory Animal Center of Nanjing Agricultural University. After a three-day acclimation period, those animals were randomly grouped into KCH (control), KMH (model), and KYH (treatment). Mice in the KMH and KYH groups were administered potassium dichromate ($K_2Cr_2O_7$) at a dose of 15 mg/kg daily via intragastric gavage to induce chromium toxicity. In addition, the KYH group received 50 mg/kg of polysaccharide of Xizang Coriolus versicolor (CV) by gavage. The KCH and KMH groups received an equivalent volume of distilled water. All mice were fed for five weeks. At the end of the experiment, the animals were euthanized using CO_2 inhalation. The body and spleen weights were recorded.

Serum examination: The blood samples collected from mice were centrifuged at 3000 ×g for 20 minutes to obtain serum for evaluating inflammatory markers and antioxidant capacity. Commercial assay kits for T-AOC, GSH-Px, SOD, MDA, IL-6, IL-10, IL-1β, and TNF-α were bought from Solarbio Science & Technology Co., Ltd. (Beijing, China).

Pathological staining analysis: Spleen tissues from the mice were preserved in polyoxymethylene (4%), and histological staining with H&E and Sirius Red was performed at Wuhai Pinuofei Biological Technology (China). Pathological examinations were conducted using a microscope (BX43, Olympus Co., Japan).

Microbiome sequencing: Mice's genomic DNAs were extracted from the ileal contents by employing the SteadyPure Stool DNA Extraction Kit (Accurate Biology, China). The quality and concentration of the extracted products were assessed via the Thermo NanoDrop ND-2000C spectrophotometer (Thermo Fisher Scientific, USA) and confirmed by 1.5% agarose gel. DNA samples that met quality standards were applied for 16S rRNA (V3–V4) gene amplification using the 338F/806R primer pair (Peng *et al.,* 2024; Xu *et al.,* 2025). The resulting amplicons were purified by piloting the GenElute Gel Extraction Kit (Yeasen, China) and subjected to high-throughput sequencing on the Illumina MiSeq platform at Wuhan Bioyi Biotechnology Co., Ltd.

Sequence analysis: The raw sequencing data of each mouse group were quality-filtered by utilizing the DADA2 plugin (Okoro *et al.,* 2023). Following quality control, non-singleton amplicon sequence variants were produced by aligning the filtered reads using the Raft algorithm. The shared and unique ASVs among the KCH, KMH, and KYH groups were visualized using a Venn diagram generated with the R package, as described previously (Xiao *et al.,* 2022). Alpha diversity indices included Faith's Phylogenetic Diversity (PD), Chao1, Pielou's evenness, Shannon index, Good's coverage, Simpson index, and Observed species. For beta diversity, Unweighted Pair Group Method with Arithmetic Mean (UPGMA), Principal

Coordinates Analysis (PcoA), Non-metric Multidimensional Scaling (NMDS), and Principal Component Analysis (PCA) were applied. Microbiota composition differences among different animal groups were examined through Linear Discriminant Analysis, Effect Size, and t-tests. Besides, PICRUSt2 was employed to predict the microbiota function of mice in different groups by blasting the database of MetaCyc and KEGG.

Statistical analysis: Data from the KCH, KMH, and KYH groups were compared via one-way ANOVA followed by Dunnett's post hoc test (SPSS, 27.0). Results of mice are depicted as means ± standard deviation (SD). P-value <0.05 was recognized as statistically significant.

RESULTS

CV polysaccharide mitigated mice damage caused by hexavalent chromium: In the current study, animals in the KMH group presented slightly lower body weight compared to those in the KCH and KYH groups. Notably, on day 35, the body weight of KMH mice was significantly lower than that of mice in KCH (P<0.05) and KYH (P<0.05) groups (Fig. 1a). Conversely, the spleen index in KMH mice was significantly higher than that of other mouse groups (P<0.05) (Fig. 1b).

Histological analysis using H&E and Sirius red staining showed that hexavalent chromium led to pronounced atrophy of white pulp and acini lienal, blurry marginal zone, infiltration of inflammatory cells, and fibration in mice, especially in the spleen tunica area. However, mice supplemented with CV polysaccharide displayed well-defined red and white pulp, reduced inflammatory cells, and decreased fibrosis (Fig. 1c).

Serum biochemical indices analysis in mice exposed to hexavalent chromium: Inflammatory cytokines IL-6 (P<0.01), IL-1β (P<0.001), and TNF-α (P<0.001) were observably elevated in hexavalent chromium-treated mice (KMH group), whereas the cytokine IL-10 was markedly reduced (P<0.01). Oxidative stress markers also showed notable changes: total antioxidant capacity (T-AOC, P<0.001) and glutathione peroxidase (GSH-Px, P<0.001) levels were significantly decreased, while malondialdehyde (MDA, P<0.001) levels were significantly increased in the KMH group. Remarkably, treatment with CV polysaccharide significantly reduced levels of IL-6 (P<0.01), IL-1β (P<0.001), TNF-α (P<0.01), and MDA (P<0.001), while significantly enhancing T-AOC (P<0.01) and GSH-Px (P<0.001) levels in mice (Fig. 2a&b).

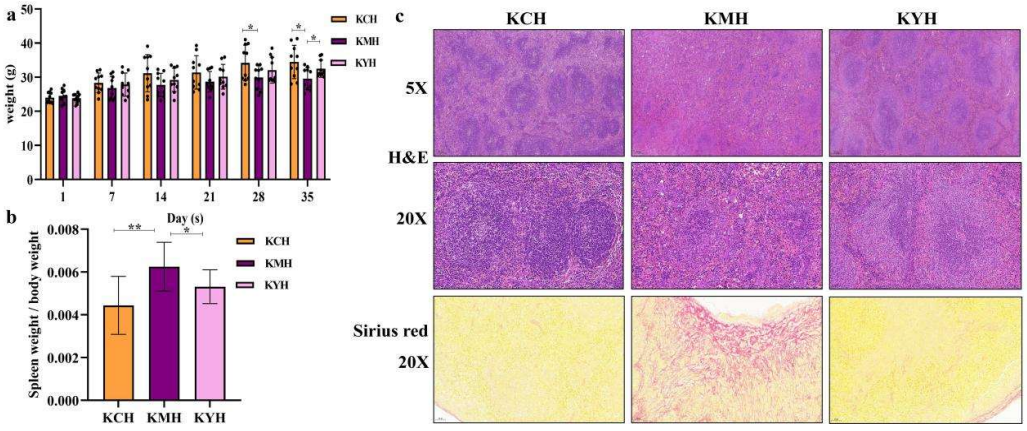

Fig. 1: CV polysaccharide decreased the damage caused by hexavalent chromium. a: Body weight, b: Spleen index. c: Pathological examination. Data were presented as the mean ± SEM. *P<0.05 and **P<0.01.

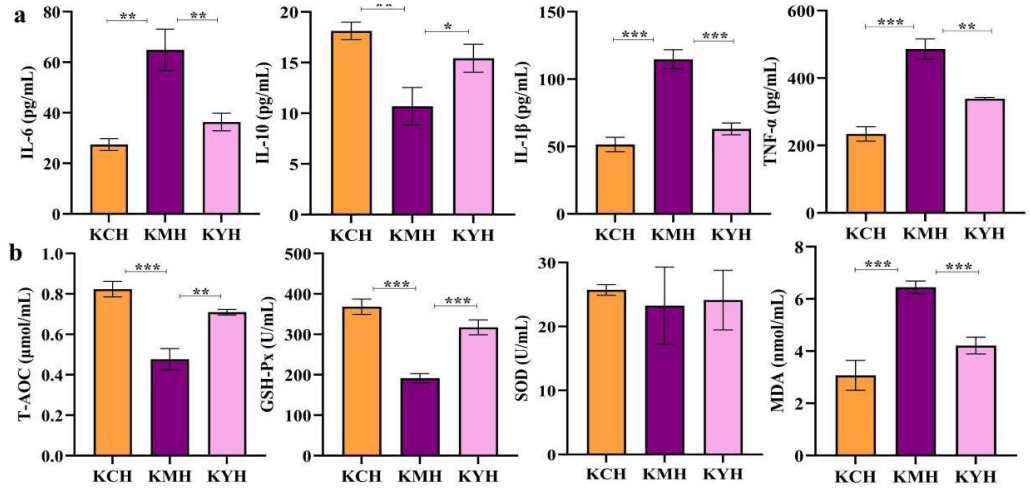

Fig. 2: The effect of CV polysaccharide on serum biochemical indices in mice induced by hexavalent chromium. a: Inflammatory factor, b: Antioxidant enzymes. Significance is indicated as *P<0.05, **P<0.01, ***P<0.001, and ****P<0.0001. Data were presented as the mean ± SEM.

The effect of CV polysaccharide on sequences and alpha diversity in mice challenged by hexavalent chromium: A total of 516,684 (KCH), 488,126 (KMH), and 483,852 (KYH) raw sequences were obtained from mice in each group, and after quality filtering, 480,057 (KCH), 453,135 (KMH), and 450,209 (KYH) high-quality sequences remained (Table 1). The rarefaction curves plateaued rapidly (Fig. 3a), indicating sufficient sequencing depth. Species accumulation curves showed a slight upward trend with increasing sample size (Fig. 3b), and the rank abundance curves displayed flat, horizontal profiles (Fig. 3c), suggesting good species evenness and diversity in the intestinal microbiota. No significant difference in alpha diversity indices was observed in different animal groups (Table 2, Fig. 3d).

Table 1: The sequence information of mice in the KCH, KMH, and KYH groups

Samples	Input	Filtered	Denoised	Merged	Non-chimeric
KCH1	87756	81560	80676	77002	52357
KCH2	87458	81376	80592	76246	45827
KCH3	83845	77417	76539	71678	45121
KCH4	95559	89210	88686	86877	69270
KCH5	74027	68896	67466	59972	42169
KCH6	88039	81598	81084	79070	63476
KMH1	89593	82697	82259	77687	45729
KMH2	73352	68070	67108	62974	51039
KMH3	84318	78155	77207	70201	42573
KMH4	73027	68026	67502	64935	49706
KMH5	76914	72219	71880	71044	56380
KMH6	90922	83968	83120	77329	37303
KYH1	96632	90184	88259	78653	52992
KYH2	65152	60388	59657	56970	43336
KYH3	89797	83813	82526	75938	46454
KYH4	72083	67099	66525	63606	41970
KYH5	81402	75480	74694	70606	45947
KYH6	78786	73245	72349	68307	54747

CV polysaccharide restored intestine microbiota composition in hexavalent chromium-induced mice: There were 175 ASVs found to be shared among the KCH, KMH, and KYH groups (Fig. 4a). At the phylum level, Firmicutes_D, Firmicutes_A, and Actinobacteriota were the predominant taxa in both the KCH (50.48%, 38.82%, and 5.08%, respectively) and KMH (77.55%, 10.91%, and 7.50%, respectively) groups. In contrast, the KYH group was primarily dominated by Firmicutes_D (66.31%), followed by Firmicutes_A (9.27%) and Bacteroidota (8.70%) (Fig. 4b). At the class level, the predominant bacterial classes in the KCH group were Bacilli (50.49%), Clostridia_258483 (38.82%), and Bacteroidia (4.74%). In the KMH group, Bacilli (77.55%), Clostridia_258483 (10.91%), and Actinomycetia (7.32%) were the dominant classes. Similarly, the KYH group was primarily composed of Bacilli (66.31%), Clostridia_258483 (9.23%), and Bacteroidia (8.70%) (Fig. 4c). At the order level, the predominant bacterial orders in the KCH group were Lactobacillales (43.83%), Clostridiales (36.31%), and Staphylococcales (6.37%). In the KMH group, Lactobacillales (70.35%) remained dominant, followed by Clostridiales (10.17%) and Staphylococcales (6.12%). Conversely, the KYH group showed a distinct microbial profile, with Lactobacillales (64.33%), Bacteroidales (8.72%), and Verrucomicrobiales (8.70%) being the leading orders (Fig. 4d). At the family level, Lactobacillaceae (41.60%), Clostridiaceae_222000 (36.37%), and Eggerthellaceae (4.19%) were predominant in KCH. In KMH, the most abundant families included Lactobacillaceae (66.62%), Clostridiaceae_222000 (10.21%), and Muribaculaceae (1.57%). In KYH, Lactobacillaceae (55.32%), Akkermansiaceae (8.70%), and Muribaculaceae (8.67%) were the primary families observed (Fig. 4e). At the genus level, the KCH group was mainly composed of *Lactobacillus* (23.37%), *Dwaynesavagella* (29.13%), and *Limosilactobacillus* (18.88%). In KMH, *Limosilactobacillus* (36.17%), *Lactobacillus* (23.34%), and *Ligilactobacillus* (9.10%) were dominant. Meanwhile, the KYH group exhibited microbial community rich in *Lactobacillus* (34.59%), *Limosilactobacillus* (22.45%), and *Akkermansia* (9.02%) (Fig. 4f).

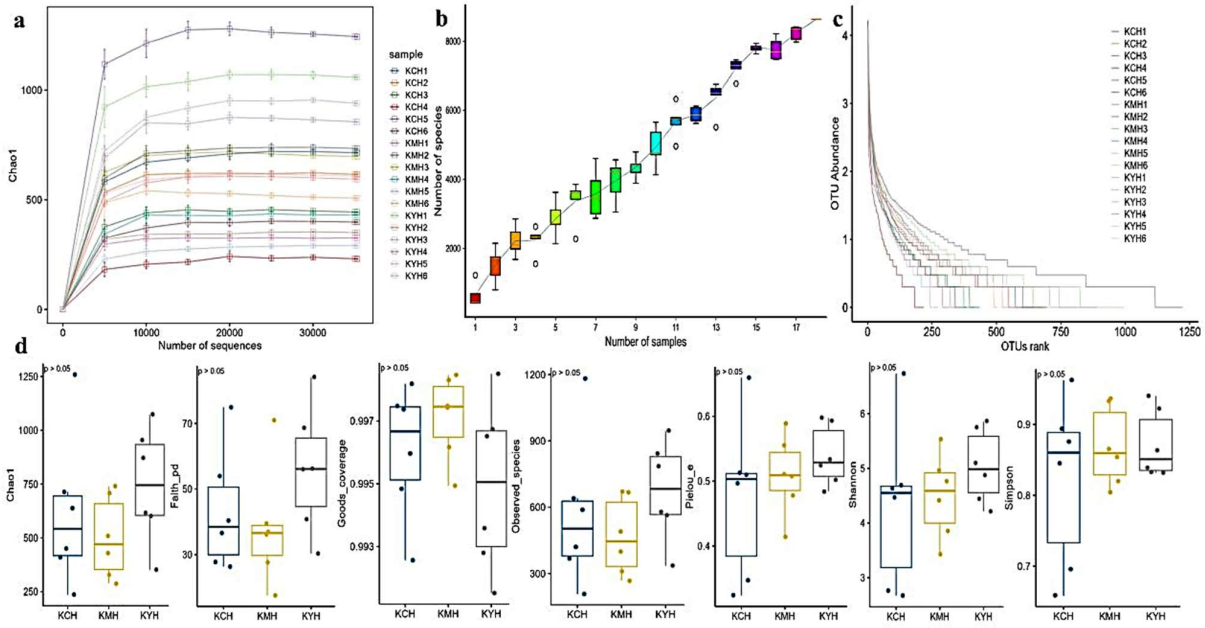

Fig 3: Alpha diversity analysis of mice in KCH, KMH, and KYH groups. a: Rarefaction curve, b: Species accumulation curves, c: Rank abundance curve, d: Alpha diversity indexes comparing analysis.

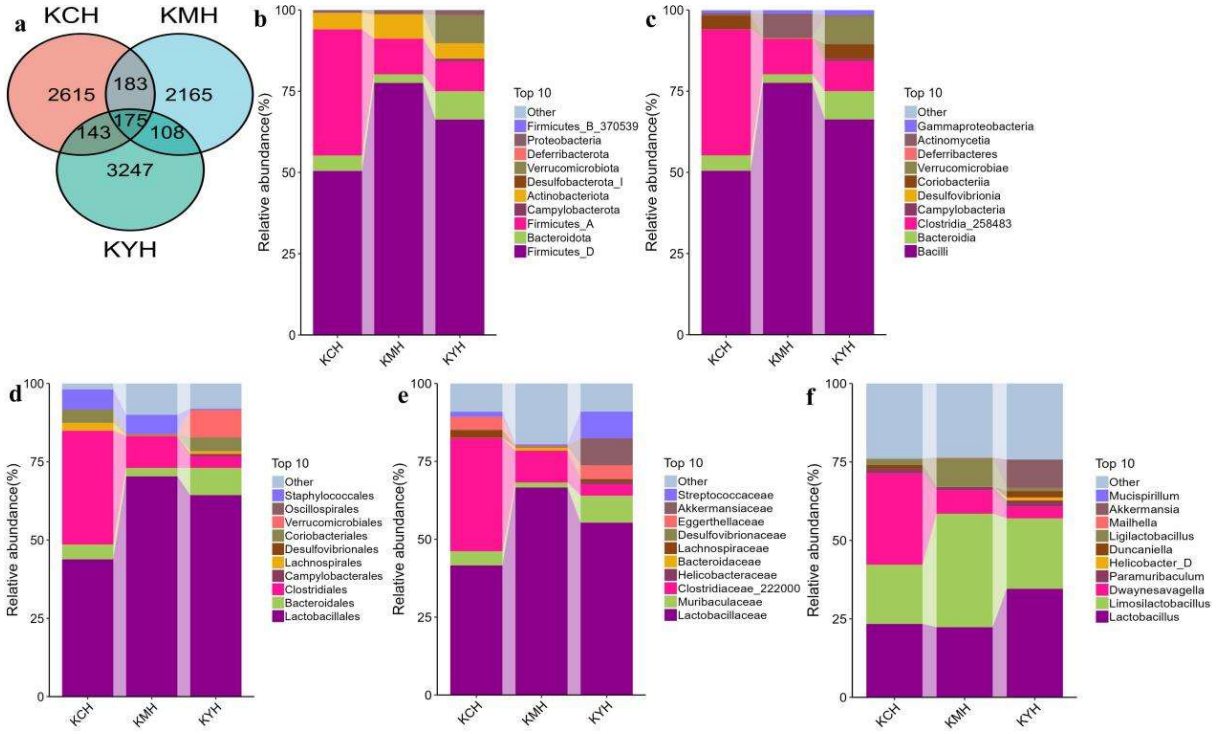

Fig. 4: The effect of CV polysaccharide on the microbiota composition in mice induced by hexavalent chromium. a: Venn map, b: Phylum, c: Class, d: Order, e: Family, f: Genus.

Table 2: Comparing the analysis of alpha diversity in mice in different groups.

Sample	Chao1	Faith_pd	Goods_coverage	Observed_species	Pielou_e	Shannon	Simpson
KCH1	714.4312409	53.9788895	0.994840762	641	0.496942931	4.63356711	0.845515535
KCH2	635.8879656	40.33161147	0.995963289	587.2	0.509240705	4.683796192	0.874948478
KCH3	448.3968528	36.57578501	0.997371019	419.3	0.512448798	4.464335012	0.893335894
KCH4	235.3976768	26.3062366	0.998182749	206.9	0.346889039	2.668462845	0.695342012
KCH5	1258.425637	74.97138769	0.992562799	1181.9	0.659368571	6.730071105	0.962504324
KCH6	407.2657663	27.69626482	0.997473399	366.3	0.323670435	2.756627859	0.657913366
KMH1	327.8247664	27.59115333	0.99830311	309.7	0.41396932	3.425461771	0.804096761
KMH2	739.6319257	70.99007617	0.994935829	666.6	0.507357242	4.759333178	0.853736335
KMH3	707.8767018	37.00882699	0.99616805	670.8	0.588839433	5.529033593	0.936662814
KMH4	428.9588062	39.45339318	0.997480712	399.1	0.510652372	4.412288417	0.865174673
KMH5	288.2269769	17.53991477	0.998467951	267.8	0.478185168	3.856526944	0.820436945
KMH6	511.0096579	36.13423742	0.997429522	491.5	0.555540365	4.967082187	0.933966983
KYH1	1072.299183	84.18890322	0.991517057	945.4	0.592680055	5.858489139	0.921636377
KYH2	599.7990612	56.2102274	0.996738455	562.5	0.533066079	4.869895218	0.862831162
KYH3	871.2199352	68.68603268	0.993586603	785.2	0.597624115	5.747287662	0.940104925
KYH4	350.7585579	30.28010297	0.998500859	335	0.501735498	4.208514644	0.831443633
KYH5	618.9115146	40.84493159	0.996519068	580.6	0.484430786	4.447730067	0.83373403

Distinct Bacterial Taxa in Mice Treated with CV Polysaccharide: Beta diversity analysis forecasts no remarkable differences in the overall microbial community composition among the KCH, KMH, and KYH groups (Fig. 5a). However, a detailed heatmap analysis revealed distinct variations of specific bacterial taxa across groups. At the phylum level, *Chloroflexota*, *Firmicutes A*, *Firmicutes B_370539*, *Patescibacteria*, and *Nitrospirota A_437815* were enriched in mice in KCH. The KYH group exhibited higher abundances of *Campylobacterota*, *Verrucomicrobiota*, *Firmicutes G*, *Acidobacteriota*, *Bacteroidota*, *Cyanobacteria*, and *Proteobacteria*. Meanwhile, animals in KMH were characterized by raised abundances of *Actinobacteriota* and *Desulfobacterota I* (Fig. 5b).

At the genus level, the KMH group showed increased abundance of *Prevotella*, *Cryptobacteroides*, *Limosilactobacillus*, *Lawsonibacter*, *Ligilactobacillus*, *Corynebacterium*, *Facklamia A_322620*, *Alloprevotella*, *Phocaeicola A_858004*, *Bacteroides H*, *Parabacteroides B_862066*, *Mailhella*, and *Desulfovibrio R_446353*. In contrast, the KYH group had higher levels of *Romboutsia B*, *Lactobacillus*, *UBA9715*, *Streptococcus*, *Kineothrix*, *UMGS1994*, *Helicobacter D*, *Dubosiella*, *Muribaculum*, *Akkermansia*, *Helicobacter C_479931*, and *Eubacterium R*. The KCH group was enriched in *Gemella*, *Clostridium T*, *Mammaliicoccus_319276*, *Dwaynesavagella*, *CAG-873*, *UBA3282*, *UBA3263*, and *COE1* (Fig. 5b).

LEfSe showed that Lactococcus A 343473 (P<0.05), Streptococcusdanieliae (P<0.05), Coriobacteriia (P<0.05), Coriobacteriales (P<0.05), Eggerthellaceae (P<0.05), Clostridium Tparaputrificum 208099 (P<0.05), Clostridium T (P<0.05), Clostridiaceae 222000 (P<0.05), Firmicutes A (P<0.05), Clostridia 258483 (P<0.05) and Dwaynesavagella (P<0.05) were significantly higher in KCH. Staphylococcal (P<0.05), *Staphylococcus equorum*

(P<0.05), and Staphylococcus (P<0.05) were noticeably higher in KMH. The KYH group presented a significantly higher abundance of UBA7173 (P<0.01), Akkermansiamuciniphila (P<0.01), Verrucomicrobiota (P<0.01), Verrucomicrobiae (P<0.01), Verrucomicrobiae (P<0.01), Akkermansiaceae (P<0.01), Akkermansia (P<0.01), UBA9715 (P<0.01), Peptostreptococcales (P<0.05), Peptostreptococcaceae (P<0.05), D16 (P<0.05), Parasutterellasp (P<0.05), Burkholderiales (P<0.05), Burkholderiaceae A (P<0.05), Burkholderiaceae (P<0.05), Duncaniella (P<0.05), Paramuribaculum (P<0.05), Lactobacillus (P<0.05), Streptococcaceae (P<0.05), Muribaculumgordoncarteri (P<0.05), Adlercreutzia 404257 (P<0.05), CAG 485 (P<0.05), QWKK01 (P<0.05) and Lactobacillus intestinalis (P<0.05) (Fig. 6).

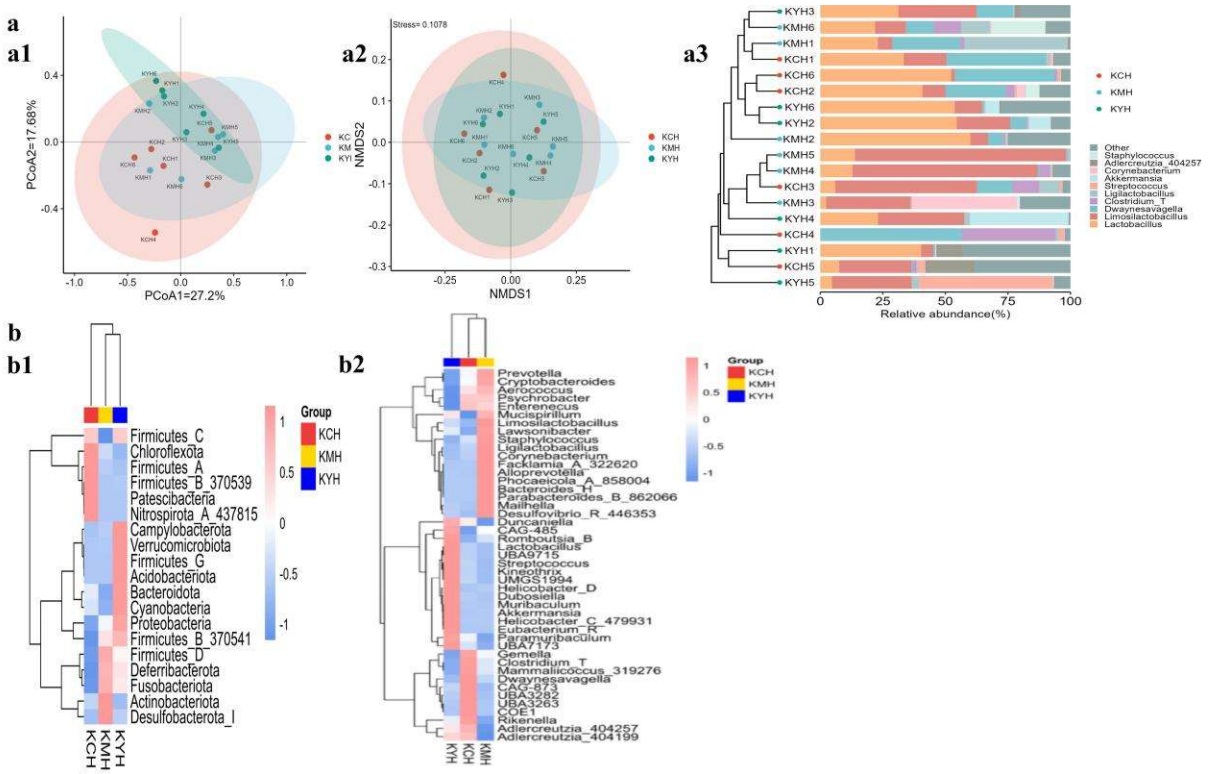

Fig. 5: The effect of CV polysaccharide on beta diversity and microbiota structure via heat map analysis of mice induced by hexavalent chromium. a: Beta diversity (a1: PCoA, a2: NMDS, a3: UPGMA clustering analysis), b: Heat map (b1: Phylum, b2: Genus).

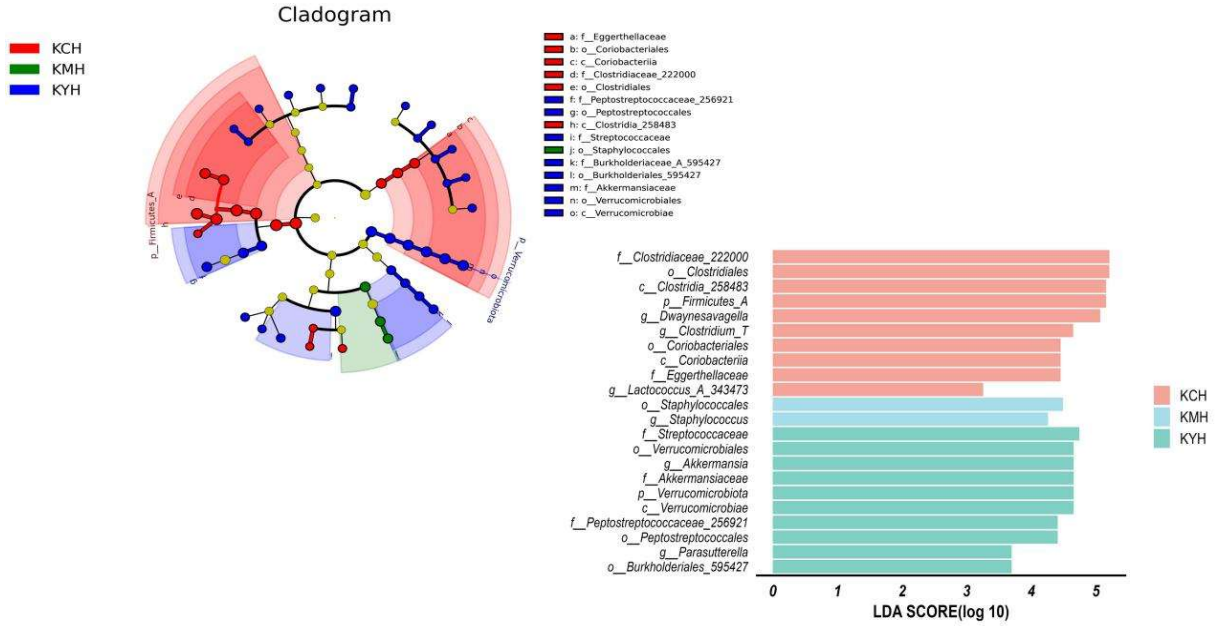

Fig. 6: Differentially abundant bacterial taxa in CV polysaccharide-treated mice exposed to hexavalent chromium, identified using LEfSe analysis.

T-test analysis showed that Firmicutes A was observably higher in the KCH group compared to both KMH and KYH (P<0.05). Cyanobacteria were significantly higher in KYH than KMH (P<0.01) (Fig. 7a). *Dwaynesavagella* and *COE1* were markedly enriched in KCH compared to both KMH and KYH (P<0.05). *Streptococcus* was also significantly higher in KCH compared to KMH (P<0.05). In the KYH group, UBA7173, QWKK01, and Bifidobacterium_388775 were significantly higher than in KMH (P<0.05). Conversely, *Lactococcus A_343473* was significantly higher in KMH compared to KYH (P<0.05). Additionally, *Gemella* and *Bacillus P_294101* were more abundant in KCH compared to KYH (P<0.05) (Fig. 7b).

CV polysaccharide altered microbiota function in mice exposed to hexavalent chromium: KEGG pathway analysis revealed significant differences in microbial functional profiles among the treatment groups (Fig. 8a). In the KCH group, pathways related to bacterial chemotaxis (P<0.05), flagellar assembly (P<0.05), plant–pathogen interaction (P<0.05), the two-component system, and beta-alanine metabolism were significantly enriched. In contrast, the KMH group showed higher representation of pathways involved in aminobenzoate degradation (P<0.01), benzoate degradation (P<0.05), chlorocyclohexane and chlorobenzene degradation (P<0.05), fatty acid metabolism (P<0.05), taurine and hypotaurine metabolism (P<0.05), and tyrosine metabolism (P<0.05). Notably, the RNA degradation pathway was dramatically higher than the KYH group (P<0.05) (Fig. 8a).

MetaCyc analysis showed that ARO-PWY (P<0.05), CENTFERM-PWY (P<0.05), COMPLETE-ARO-PWY (P<0.05), LEU-DEG2-PWY (P<0.05), NONMEVIPP-PWY (P<0.05), PWY-4361 (P<0.05), PWY-5121 (P<0.05), PWY-5676 (P<0.05), PWY-6163 (P<0.01), PWY-6590 (P<0.05), and PWY-7560 (P<0.05) were significantly enriched in the KCH group. The KETOGLUCONMET-PWY pathway was markedly higher in the KMH group (P<0.05), while FERMENTATION-PWY (P<0.05), P108-PWY (P<0.05), PWY0-1241 (P<0.05), and THISYN-PWY (P<0.05) were notably elevated in the KYH group (Fig. 8b).

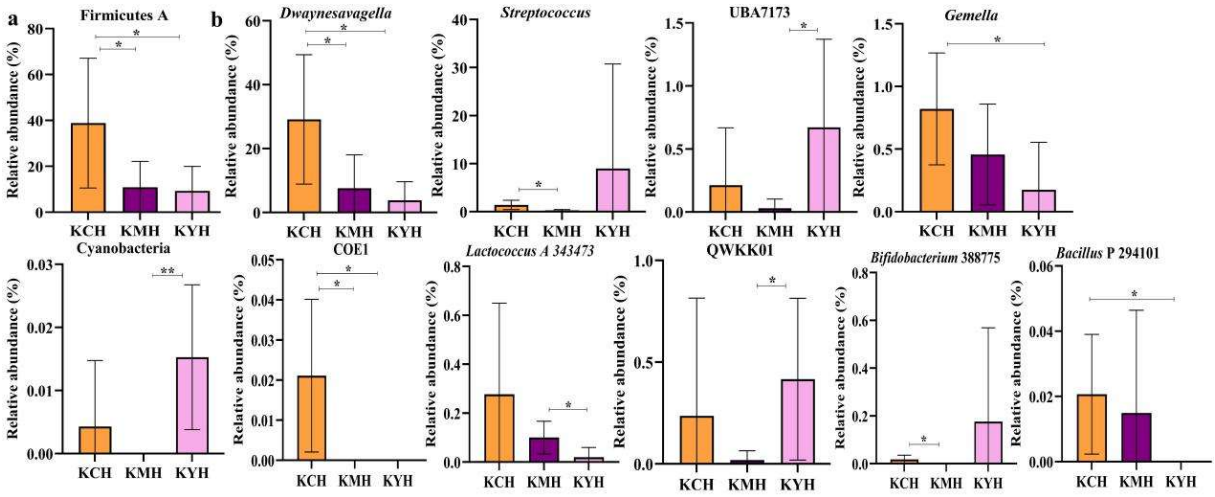

Fig. 7: Marker bacterial species in hexavalent chromium-exposed mice treated with CV polysaccharide, identified through T-test. a: Phylum, b: Genus.

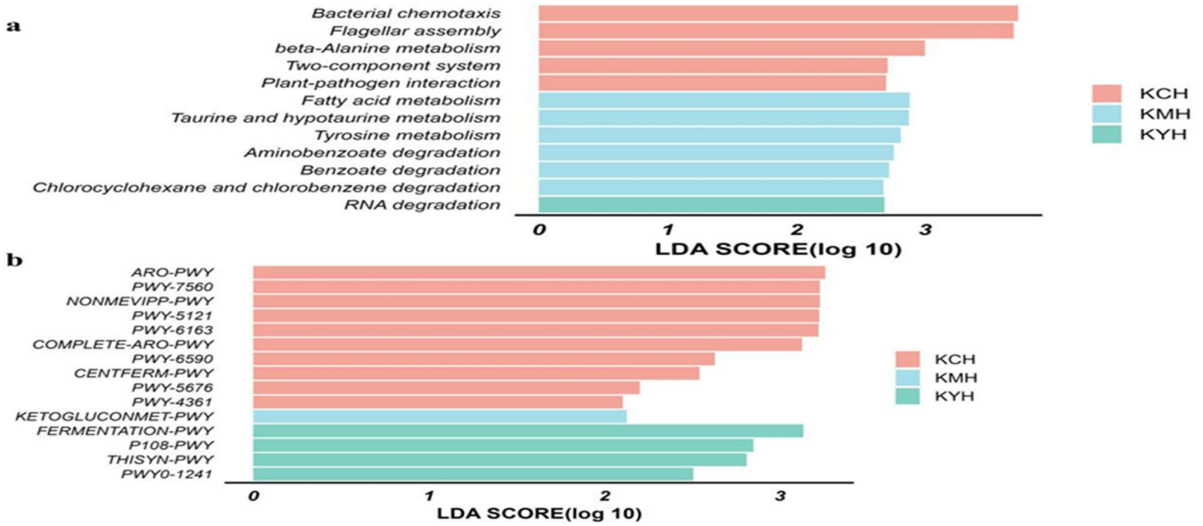

Fig. 8: Function analysis of CV polysaccharide-treated mice induced by hexavalent chromium. a: KEGG, b: MetaCyc.

DISCUSSION

The spleen is a vital immune organ; however, exposure to environmental and dietary contaminants such as chromium poses a remarkable threat to its function. In the present study, we evaluated the protective effect of the polysaccharide of Xizang *Coriolus versicolor* (CV) against chromium-induced spleen damage in mice.

Consistent with previous studies, chromium exposure led to a decrease in weight and an increase in the spleen organ index in treated animals (Chen *et al.,* 2017; Cao *et al.,* 2024; Nauroze *et al.,* 2024). In contrast, administration of CV polysaccharide promoted weight gain and reduced spleen enlargement. Histopathological analysis revealed that chromium induced spleen cell death and fibrosis, similar to findings observed in heavy metal-exposed ducks (Tang *et al.,* 2022). Interestingly, CV polysaccharide alleviated spleen damage and fibrosis in mice.

Oxidative stress is a condition of redox imbalance that leads to cellular apoptosis and tissue damage in the host (Wang *et al.,* 2025). GSH-Px and SOD are key antioxidant enzymes, while T-AOC represents the overall antioxidant potential. MDA, on the other hand, reflects the level of oxidative damage (Hu *et al.,* 2023). These four markers are widely employed to evaluate oxidative stress. In chromium-exposed mice, decreased T-AOC and GSH-Px, along with elevated MDA, were observed, in compliance with previous findings (Wang *et al.,* 2023; Alwaili *et al.,* 2024). Treatment with Coriolus versicolor (CV) polysaccharide significantly increased T-AOC and GSH-Px levels and reduced MDA levels, suggesting that it mitigates oxidative damage by enhancing the antioxidant defense system.

IL-6, IL-1β, and TNF-α are proinflammatory cytokines involved in pathological processes (Zheng *et al.,* 2023), while IL-10 is an important anti-inflammatory cytokine suppressing inflammatory reaction (York *et al.,* 2024). The higher levels of IL-6, IL-1β, and TNF-α, and lower IL-10 in chromium-challenged mice were in line with ducks treated with chromium (Xing *et al.,* 2022). However, CV polysaccharide treatment reversed these trends by upregulating IL-10 and downregulating proinflammatory cytokines, indicating its protective role in reducing tissue injury through modulation of the inflammatory response.

Subsequently, we performed microbiota sequencing and obtained 1,383,401 high-quality filtered sequences (Table 1). No significant differences in alpha diversity were found among the different groups, which contrasts with findings from studies involving hexavalent chromium-exposed Bufo gargarizans tadpoles (Yao *et al.,* 2019), and mice (Mu *et al.,* 2023). However, notable alterations in microbial composition and functional profiles were detected across different taxa. Interestingly, CV polysaccharide treatment partially restored the gut microbiota structure in mice. For instance, *Lactobacillus* was the dominant genus in both KCH and KYH groups, whereas *Limosilactobacillus* was predominant in the KMH group. *Lactobacillus* is a well-known probiotic genus commonly isolated from healthy hosts, recognized for its immunomodulatory properties and its role in maintaining intestinal homeostasis (Du *et al.,* 2022). The increased abundance of *Lactobacillus* in CV polysaccharide-supplemented mice showed that CV polysaccharide could promote probiotic bacterial proliferation.

Further taxonomic analysis revealed prominent differences in two phyla and nine genera among the three groups. Those genera were *Dwaynesavagella*, *Streptococcus*, *UBA7173*, *QWKK01*, *Bifidobacterium* 388775, *Lactococcus* A 343473, *Gemella,* and *Bacillus* P 294101. *Streptococcus* is a primary genus in healthy hosts (Bloch *et al.,* 2024), and some *Streptococcus* species, like strain D19 and *Streptococcus salivarius* strains, are probiotic bacteria (Gurbanov *et al.,* 2021; Zhang and Xiao, 2023). Its increased abundance in the KCH and KYH groups suggests a possible association with the therapeutic effects of CV polysaccharide. Similarly, members of the *Bifidobacterium* genus are well-recognized probiotics that confer various health benefits (Schlienger De Alba and Espinosa Andrews, 2024). Notably, *Bifidobacterium* can produce lactic acid derivatives that enhance immune function, particularly in infants (Laursen *et al.,* 2021). The increased abundance of *Bifidobacterium* 388775 in CV polysaccharide-treated mice showed that this polysaccharide could contribute to the colonization of beneficial bacteria in animals.

Conclusions: In summary, our findings demonstrate that *Coriolus versicolor* polysaccharide alleviates chromium-induced spleen damage in mice by modulating inflammatory responses, enhancing antioxidant capacity, and restoring gut microbiota balance. The current study highlights the promising potential of polysaccharide of Xizang *Coriolus versicolor* as a natural therapeutic agent against heavy metal-induced organ damage, particularly targeting chromium-induced spleen toxicity.

Data availability statement: All the generated sequence data were deposited in the NCBI database under accession number: PRJNA1246584.

Authors contribution: KL, YH, and SC: research idea and methodology. SC, CX, QH, QL, and MA: reagents, materials, and analysis tools. SC, YH and KL: writing – original draft and preparation. MAM, EAA, KL and YH: writing – review and editing. KL: visualization and supervision. All authors know and approve the final manuscript.

Acknowledgments: This research was funded by Natural Science Foundation of Hubei Province: The mechanism of action of the traditional Chinese medicine prescription Qingyu Hejiang Decoction in the treatment of reflux esophagitis based on microbiota-metabolomics research (2022CFD141).

The authors acknowledge the Princess Nourah bint Abdulrahman University Researchers Supporting project number: (PNURSP2026R224), Princess Nourah bint Abdulrahman University, Riyadh, Saudi Arabia. The authors extend their appreciation to the Deanship of Research and Graduate Studies at King Khalid University for funding this work through Large Research Project under grant number RGP2/223/46.

Conflicts of Interest: The authors declare no conflict of interest.

REFERENCES

Albhaisi SA, Bajaj JS and Sanyal AJ, 2019. Role of gut microbiota in liver disease. American Journal of Physiology, Gastrointestinal Liver Physiology (318(1):G84-G98.

Aljohani ASM, 2025. Chromium and nickel toxicity in sheep: pathophysiology and management approaches. Pakistan Veterinary Journal 45(1): 62-72.

Alipour R, Marzabadi LR, Arjmand B, *et al*., 2022. The effects of medicinal herbs on gut microbiota and metabolic factors in obesity models: A systematic review. Diabetes & Metabolic Syndrome: Clinical Research Reviews 16(9):102586.

Alwaili MA, Elhoby AH, El-Sayed NM, *et al*., 2024. Cardioprotective effects of alpha-Asarone against Hexavalent Chromium-induced oxidative damage in mice. Drug Design Development and Therapy 18:3383-3397.

Bloch S, Hager-Mair FF, Andrukhov O, *et al*., 2024. Oral streptococci: modulators of health and disease. Frontiers in Cell Infection and Microbiology 14:1357631-1357631.

Boşgelmez İİ and Güvendik G, 2019. Beneficial Effects of N-Acetyl-L-cysteine or Taurine pre- or post-treatments in the heart, spleen, lung, and testis of Hexavalent Chromium-exposed mice. Biological Trace Element Research 190(2):437-445.

Bronte V and Pittet MJ, 2023. The spleen in local and systemic regulation of immunity. Immunity (Cambridge, Mass.) 56(5):1152-1152.

Cao X, Zheng S, Zeng Y, *et al*., 2024. Effects of chronic Cr and Ni co-exposure on liver inflammation and autophagy in mice by regulating the TLR4/mTOR pathway. Science of the Total Environment 926:171921.

Chen F, Huang G, Yang Z, *et al*., 2019. Antioxidant activity of *Momordica charantia* polysaccharide and its derivatives. International Journal of Biological Macromolecules 138:673-680.

Chen P, Zhu Y, Wan H, *et al*., 2017. Effects of the oral administration of K2Cr2O7 and Na2SeO3 on Ca, Mg, Mn, Fe, Cu, and Zn contents in the heart, liver, spleen, and kidney of chickens. Biological Trace Element Research 180(2):285-296.

Du T, Lei A, Zhang N, *et al.,* 2022. The beneficial role of probiotic Lactobacillus in respiratory diseases. Frontiers in Immunology 13:908010-908010.

El-Sayed A, Aleya L and Kamel M, 2021. Microbiota's role in health and diseases. Environmental Science and Pollution Research 28(28):36967-36983.

Geng J, Ni Q, Sun W, *et al*., 2022. The links between gut microbiota and obesity and obesity related diseases. Biomedicine and Pharmacotherapy 147:112678.

Gurbanov R, Karadağ H, Karaçam S, *et al.,* 2021. Tapioca starch modulates cellular events in oral probiotic *Streptococcus salivarius* strains. Probiotics and Antimicrobial Proteins 13(1):195-207.

Hu W, He Z, Du L, *et al*., 2023. Biomarkers of oxidative stress in broiler chickens attacked by lipopolysaccharide: A systematic review and meta-analysis. Ecotoxicology and Environmental Safety 266:115606.

Jeitler M, Michalsen A, Frings D, *et al*., 2020. Significance of medicinal mushrooms in integrative oncology: A Narrative Review. Frontiers in Pharmacology 11:580656.

Jing Y, Zhang S, Li M *et al*., 2022. Research progress on the extraction, structure, and bioactivities of polysaccharides from *Coriolus versicolor*. Foods 11(14):2126.

Kim J, Kim Y, and Kumar V, 2019. Heavy metal toxicity: An update of chelating therapeutic strategies. Journal of Trace Elements in Medicine and Biology 54:226-231.

Laursen MF, Sakanaka M, Von Burg, N *et al*., 2021. Bifidobacterium species associated with breastfeeding produce aromatic lactic acids in the infant gut. Nature Microbiology 6(11):1367-1382.

Luo K, Yue GG, Ko C, *et al*., 2014. *In-vivo* and *in-vitro* anti-tumor and anti-metastasis effects of Coriolus versicolor aqueous extract on mouse mammary 4T1 carcinoma. Phytomedicine 21(8-9):1078-1087.

Ma Y, Li S, Ye S, *et al*., 2022. Hexavalent chromium triggers hepatocytes premature senescence via the GATA4/NF-κB signaling pathway mediated by the DNA damage response. Ecotoxicology and Environmental Safety 239:113645.

Mu J, Guo Z, Wang X, *et al*., 2023. Seaweed polysaccharide relieves hexavalent chromium-induced gut microbial homeostasis. Frontiers in Microbiology 13:1100988.

Nauroze T, Ali S, Andleeb S, *et al*., 2024. Therapeutic potential of *Aloe vera* and *Aloe vera*–conjugated Silver Nanoparticles on mice exposed to Hexavalent Chromium. Biological Trace Element Research 202(12):5580-5595.

Okoro PC, Orwoll ES, Huttenhower C, *et al*., 2023. A two-cohort study on the association between the gut microbiota and bone density, microarchitecture, and strength. Frontiers in Endocrinology 14:1237727.

Peng S, Xu C, He Q, *et al*., 2024. Fucoidan alleviates intestine damage in mice induced by LPS via regulation of microbiota. Pakistan Veterinary Journal 44(2):517-525.

Pilkington K, Wieland LS, Teng L, *et al*., 2022. Coriolus (Trametes) versicolor mushroom to reduce adverse effects from chemotherapy or radiotherapy in people with colorectal cancer. Cochrane Database Systemic Reviews 11(11):CD012053.

Saleh MH, Rashedi I and Keating A, 2017. Immunomodulatory Properties of Coriolus versicolor: The Role of Polysaccharopeptide. Frontiers in Immunology 8:1087.

Saleem M, Ali S, Javaid A, *et al.,* 2025. Antitoxic Effects of fennel (*Foeniculum vulgare*) extract against Chlorpyrifos induced toxicity in rabbits. Pakistan Journal of Veterinary and Animal Research 1(2):59-62.

Schlienger De Alba BN, and Espinosa Andrews H, 2024. Benefits and challenges of encapsulating Bifidobacterium probiotic strains with Bifidogenic prebiotics. Probiotics and Antimicrobial Proteins 16(5):1790-1800.

Sharma P, Singh SP, Parakh SK, *et al*., 2022. Health hazards of hexavalent chromium Cr (VI) and its microbial reduction. Bioengineered 13(3):4923-4938.

Sittipo P, Choi J, Lee S, *et al*., 2022. The function of gut microbiota in immune-related neurological disorders: a review. Journal of Neuroinflammation 19(1):154.

Tang L, Lan J, Jiang X, *et al*., 2022. Curcumin antagonizes inflammation and autophagy induced by arsenic trioxide through immune protection in duck spleen. Environmental Science and Pollution Research 29(50):75344-75355.

Wang C, Dai X, Xing C, *et al*., 2023. Hexavalent-Chromium-induced disruption of Mitochondrial dynamics and apoptosis in the liver via the AMPK-PGC-1α pathway in ducks. International Journal of Molecular Sciences 24(24):17241.

Wang K, Shi X, Lin H, *et al*., 2025. Selenium deficiency exacerbates ROS/ER stress mediated pyroptosis and ferroptosis induced by bisphenol A in chickens thymus. Journal of Environmental Science 148:13-26.

Wise JP, Young JL, Cai J, *et al*., 2022. Current understanding of hexavalent chromium [Cr(VI)] neurotoxicity and new perspectives. Environment International 158:106877.

Wise SS and Wise JP, 2012. Chromium and genomic stability. Mutation Research/Fundamental and Molecular Mechanisms of Mutagenesis 733(1-2):78-82.

Wu X, Zhao L, Zhao Y, *et al*., 2024. Traditional Chinese medicine improved diabetic kidney disease through targeting gut microbiota. Pharmaceutical Biology 62(1):423-435.

Xiao C, Wang Y, and Fan Y, 2022. Bioinformatics analysis identifies potential related genes in the pathogenesis of intrauterine fetal growth retardation. Evolution in Bioinformatics 18:11769343221112780.

Xu C, He Q, Zhu Z, *et al*., 2025. Propolis improves intestinal barrier function against *Cryptosporidium parvum* via NLRP6 inflammasome. mBio 16(11):e0231725.

Xing C, Yang F, Lin Y, S, *et al*., 2022. Hexavalent Chromium exposure induces intestinal barrier damage via activation of the NF-κB signaling pathway and NLRP3 inflammasome in ducks. Frontiers in Immunology 13:952639.

Yao Q, Yang H, Wang X, *et al*., 2019. Effects of hexavalent chromium on intestinal histology and microbiota in Bufo gargarizans tadpoles. Chemosphere. 216:313-323.

Yang Y, Liu Q, Li J, *et al.,* 2025. Regulation of microbiota by morel polysaccharide alleviates small intestine damage in LPS-induced mice. Pakistan Veterinary Journal 45(3):1271-1280.

York AG, Skadow MH, Oh J, Q, *et al*., 2024. IL-10 constrains sphingolipid metabolism to limit inflammation. Nature 627(8004):628-635.

Zhang M, Chen Z, Chen Q, *et al*., 2008. Investigating DNA damage in tannery workers occupationally exposed to trivalent chromium using comet assay. Mutation Research/Genetic Toxicology and Environmental Mutagenesis 654(1):45-51.

Zhang WX, and Xiao CL, 2023. Streptococcus strain D19T as a probiotic candidate to modulate oral health. BMC Microbiology 23(1):339.

Zhao Y, Hao D, Zhang H, *et al*., 2022. Selenium-enriched yeast relieves Hexavalent Chromium toxicity by inhibiting NF-κB signaling pathway in broiler spleens. Animals 12(2):146.

Zheng L, Han Z, Luo D, *et al*., 2023. IL-6, IL-1β and TNF-α regulation of the chondrocyte phenotype: a possible mechanism of haemophilic cartilage destruction. Hematology (Luxembourg) 28(1):2179867-2179867.

Zheng Y, Guan J, Wang L, *et al*., 2022. Comparative proteomic analysis of spleen reveals key immune-related proteins in the yak (Bos grunniens) at different growth stages. Comparative Biochemistry and Physiology Part D: Genomics and Proteomics 42:100968.